Modeling of optical detection of spin-polarized carrier injection into light-emitting devices

M. C. de Oliveira[1] and He Bi Sun[2,3]

[1]*Departamento de Física, CCET, Universidade Federal de São Carlos, 13565-905, São Carlos, SP, Brazil*
[2]*School of Physical Sciences, The University of Queensland, QLD 4072, Brisbane, Australia*
[3]*Special Research Centre for Quantum Computer Technology, The University of Queensland, QLD 4072, Brisbane, Australia*
(Received 2 October 2003; published 26 February 2004)

We investigate the emission of multimodal polarized light from light emitting devices due to spin-aligned carrier injection. The results are derived through operator Langevin equations, which include thermal and carrier-injection fluctuations, as well as nonradiative recombination and electronic g-factor temperature dependence. We study the dynamics of the optoelectronic processes and show how the temperature-dependent g factor and magnetic field affect the degree of polarization of the emitted light. In addition, at high temperatures, thermal fluctuation reduces the efficiency of the optoelectronic detection method for measuring the degree of spin polarization of carrier injection into nonmagnetic semicondutors.

I. INTRODUCTION

Advances on control of spin degree of freedom in electronic devices has led to a strong research program in a new branch of technology, so-called spintronics, extending the usual electronics.[1] Potential applications such as spin transistors[2] or spin memory storage devices[3-5] are among the main motivations for such a technological challenge. Since spin decoherence time is much longer than all the relevant time scales,[4] a more ambitious proposal is to encode quantum bits (qubits) of information, for quantum computation protocols, on electronic spins bounded to quantum dots,[6] or to silicon implanted impurities.[7]

One main obstacle for this technological trend is to efficiently inject (and detect) spin-polarized carriers into semiconductor media through magnetic or semimagnetic contacts.[8-10] However, recent advances have been reported with remarkable achievements of efficient (up to 86%) electrical spin-polarized carrier injection[8,11-14] through a spin aligner (spin filter[15]) into a GaAs light-emitting device (LED). Despite the many specific details and variety of materials used as spin aligners, such as BeMnZnSe,[11] ZnMnSe,[13] ferromagnetic GaMnAs epilayers,[12] or double barrier resonant tunneling diode[16,17] the standard technique for detection of the efficiency of spin-polarized carrier injection is the polarization measurement of the device emitted light at low temperature. Selection rules for radiative recombination process in GaAs allow a direct relation between spin-selective injection and the emitted light polarization. However, thermal effects such as temperature dependence of the electron g factor,[18] noise due to thermal-light emission, as well as nonradiative carrier recombination may blur the detected light degree of polarization, which could cause an apparent low efficiency in spin-polarized carrier injection at higher temperatures. Thus a detailed analysis of thermal effects on the spin-polarized photon emission and detection should be included in modeling the dynamic processes.

In this paper we analyze the temperature and magnetic field dependence of the GaAs emitted light degree of polarization, considering a full quantum model for the generation of polarized light in GaAs LED in the presence of a magnetic field. Effects such as spin-polarized carrier pumping, radiative and nonradiative recombination, as well as Zeeman splitting due to the magnetic field are considered in a quantum Langevin approach.[19,20]

There is reasonable literature on transport and noise in conventional optoelectronic devices following the quantum Langevin approach, such as Refs. 19–23. Moreover, such approaches have been quite successfully applied to description of noise in nonequilibrium quantum optical processes[24-26] including those present in light generation and detection. In this paper we model the quantum processes in nonconventional spin-polarized LED's with a microscopic description. Particularly we extend the multimodal light emission treatment of Ref. 20 by considering the spin degeneracy lifting when a magnetic field is applied on the device. Such approach is quite useful for the understanding of the relevant microscopic physical processes.

We first quantify the intrinsic degree of polarization of the GaAs light emission as it is strongly affected by temperature effects. The temperature dependence of the electronic g factor is responsible for a slight decrease of the degree of polarization, once the decrease of the electronic g factor with the temperature decreases the conduction band spin-splitting sensitivity to the magnetic field. However, at higher temperatures, thermal photons are also emitted by the GaAs device, and the intrinsic degree of polarization decreases abruptly at a threshold temperature (T_c) as T_c is dependent on the spectral response of the light detector as defined in Sec. V. The effect of unbalanced spin injection is also analyzed. We develop a quite useful expression for the degree of polarization of the emitted light, which now shows a dependence on the spin-aligned carrier pumping, as well as on the radiative and the nonradiative electron-hole recombination. Since the intrinsic polarization in GaAs is opposite to that in spin-polarizing materials, it decreases the net spin-injection efficiency as reported in Refs. 11,13,14. We model the spin-polarized carrier injection by considering the spin aligner as a Brillouin paramagnet,[27] and introduce a phenomenological spin-polarized current density, which is dependent on the
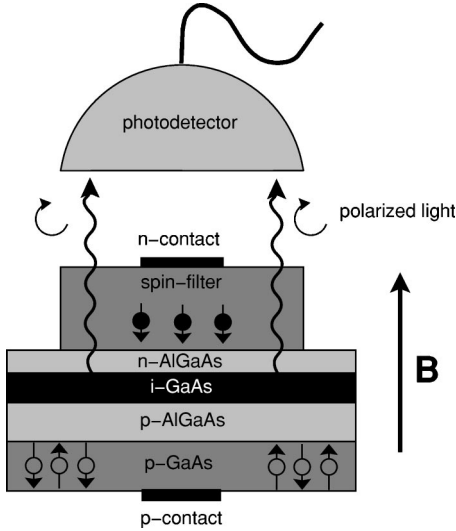
69 085322-1

FIG. 1. Spin-filtering device.

spin-aligner layer thickness, the applied magnetic field, and the temperature. We then describe the net polarized light emission due to both the intrinsic polarization of GaAs and the polarized carrier injection.

This paper is organized as follows. In Sec. II we begin with describing the model for polarized-multimode photon emission due to radiative recombination of spin-aligned carries in the active layer of GaAs LED's. In Sec. III we present the spin-polarized LED Langevin equations in a four-valence band model for the description of polarized light generation, which includes light and heavy hole-electron recombination. In Sec. IV we describe the detection process. In Sec. V we analyze the influence of temperature and magnetic field on the generation of intrinsic polarized light. In Sec. VI we present a quasiequilibrium equation for inclusion of carrier injection and nonradiative recombination. Finally in Sec. VII we discuss enclosing the paper.

II. MODEL

The system we study is depicted in Fig. 1 and is constituted by a spin-aligner material layer[8,11–13] in contact with a GaAs LED, whose emitted light is then incident on the photodetector. We model the light emission and detection of a GaAs device only, analyzing the intrinsic degree of polarization by setting each subband in quasiequilibrium with balanced injection of carriers. The spin-alignment effect is phe-
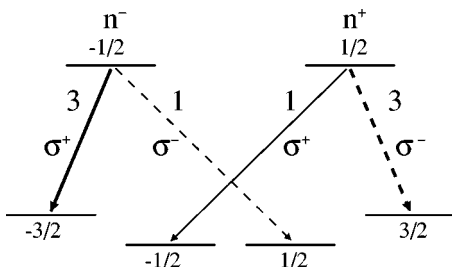

FIG. 2. Radiative interband transitions allowed in GaAs.

nomenologically considered by setting unbalanced number of carriers in each spin subband, which are in contact to fermionic reservoirs. In GaAs, the conduction band is two-fold degenerate and the valence band is fourfold degenerate (heavy and light hole spin). Spin degeneracy is lifted with a magnetic field, while the light-heavy hole degeneracy is lifted by confinement.[23,29] The allowed transitions are depicted in Fig. 2. Due to the selection rules, electrons with spin $-1/2$ in the conduction band recombine with holes of spin $-3/2$ or $1/2$ in the valence band to emit photons in right (σ^+) or left (σ^-) circular polarization, respectively. Analogously electrons with spin $1/2$ recombine with holes of spin $-1/2$ or $3/2$ to emit photons in σ^+ or σ^- polarization, respectively. In GaAs the heavy hole transition is a factor of 3 times larger than that of the light hole.

The extended model describing polarized multimode photons and carriers in the active layer of the LED in the presence of a magnetic field is given by[19,20]

$$H = H_c + H_p + H_d + H_{MB} + H_{bath} + H_{bath-sys} + H_M. \quad (1)$$

The carriers free Hamiltonian is given by

$$H_c = \sum_{\mathbf{k}} \left(\sum_{\mu} \varepsilon_{c\mathbf{k}\mu} c^{\dagger}_{\mathbf{k}\mu} c_{\mathbf{k}\mu} + \sum_{\mu'} \varepsilon_{v\mathbf{k}\mu'} d^{\dagger}_{-\mathbf{k}\mu'} d_{-\mathbf{k}\mu'} \right), \quad (2)$$

where $c_{\mathbf{k}\mu}$ and $d_{-\mathbf{k}\mu'}$ are Fermionic annihilation operators for the electron with momentum $\mathbf{k}$ and spin μ and the hole with momentum $-\mathbf{k}$ and spin μ', respectively. The spin variables are $\mu = -1/2$, $1/2$ and $\mu' = -3/2$, $-1/2$, $1/2$, $3/2$. $\varepsilon_{c\mathbf{k}\mu}$ and $\varepsilon_{v\mathbf{k}\mu'}$ are the conduction and valence band energy, respectively. The multiphotonic process is characterized by the Hamiltonian

$$H_p = \sum_{l\mu\mu'} \hbar \nu_l a^{\dagger}_{l\mu\mu'} a_{l\mu\mu'}, \quad (3)$$

with $a_{l\mu\mu'}$ and $\nu_{l\mu\mu'}$ being the bosonic annihilation operator and the frequency for the photons in mode l with the polarization characterized by the allowed spin-indexes transition μ and μ', respectively.

The dipole interaction is given by

$$H_d = \sum_{l\mathbf{k}\mu\mu'} \hbar (g_{l\mathbf{k}\mu\mu'} d^{\dagger}_{-\mathbf{k}\mu'} c^{\dagger}_{\mathbf{k}\mu} a_{l\mu\mu'} + \text{H.c.}), \quad (4)$$

where $g_{l\mathbf{k}\mu\mu'}$ is the dipole coupling constant. Notice that $\varepsilon_{c\mathbf{k}\mu}$, $\varepsilon_{v\mathbf{k}\mu'}$, and $g_{l\mathbf{k}\mu\mu'}$ are already renormalized to include the many-body interaction H_{MB} (carrier-carrier scattering) in a mean-field approximation.[19] For the direct radiative recombination in GaAs it is sufficient to consider $\varepsilon_{c\mathbf{k}\mu}$ and $\varepsilon_{v\mathbf{k}\mu'}$ in

a parabolic band structure, such as $\varepsilon_{c\mathbf{k}\mu}=\hbar^2 k^2/2m_e+\varepsilon_g$ and $\varepsilon_{v\mathbf{k}\mu'}=\hbar^2 k^2/2m_h$, where m_e is the conduction-band effective electron mass and $m_h=m_{hh},m_{lh}$ is the effective mass for the heavy and light hole, respectively; ε_g describes the renormalized band gap. To simplify the equations we have included the following zero-rate (forbidden) transition matrix elements $g_{l\mathbf{k}-1/2-1/2}=g_{l\mathbf{k}-1/23/2}=g_{l\mathbf{k}1/21/2}=g_{l\mathbf{k}1/2-3/2}\equiv 0$.

Let us choose a general orientation for the magnetic field and analyze later what transitions are allowed in the Faraday configuration, where the field is perpendicular to the layers of the device (along the z axis) as shown in Fig. 1. The action of the magnetic field over the device is described by the Zeeman Hamiltonian as[30]

$$H_M=\mu_B\mathbf{B}\cdot\sum_{\mathbf{k}}\left(\sum_{\mu\nu}\mathcal{G}_e\mathbf{S}_{c\mu\nu}c^\dagger_{\mathbf{k}\mu}c_{\mathbf{k}\nu}\right.$$

$$\left.+\sum_{\mu'\nu'}\mathcal{G}_h\mathbf{S}_{v\mu'\nu'}d^\dagger_{-\mathbf{k}\mu'}d_{-\mathbf{k}\nu'}\right),\tag{5}$$

where μ_B is the Bohr magneton, $\mathcal{G}_{e(h)}$ is the electron (hole) Landé g factor and $\mathbf{S}_c$ and $\mathbf{S}_v$ are spin 1/2 matrix for electrons and spin 3/2 for holes, respectively. In addition to lifting the spin degeneracy by introducing the Zeeman splitting, the magnetic field also induces spin-flip between carriers subbands. Although magnetic fields above 1 T are considered in this paper, since we are only interested in a qualitative view of the optical transitions close to the band edge we simplify the model by not taking into account Landau levels quantization.

In our model, the reservoir is constituted by three terms, one for the photonic modes and the other two for electrons and holes. The corresponding Hamiltonian terms ($\mathcal{H}_{\text{bath}}$ and $\mathcal{H}_{\text{bath-sys}}$) are conveniently eliminated in a Markovian approximation for the reduced dynamics of the device.[24] The photonic reservoir is assumed in a thermal distribution, while the carriers reservoir are considered in quasi-Fermi-Dirac distributions, where the carriers are in equilibrium in each subband, but not between two of them.

III. SPIN-POLARIZED LED LANGEVIN EQUATIONS

Here we consider the dynamics of the dipole operator and for the photon number operator. The interaction with the carrier reservoir is considered in the Langevin approach, which includes fluctuations in the carriers and photon populations.

The Langevin equations for the dipole operator ($\sigma^{\mu\mu'}_{\mathbf{k}}=d_{-\mathbf{k}\mu'}c_{\mathbf{k}\mu}e^{i\nu_l t}$) and for the photon annihilation operator ($A_{l\mu\mu'}=a_{l\mu\mu'}e^{i\nu_l t}$) describing the LED in a microscopic scale are given by

$$\frac{d}{dt}\sigma^{\mu\mu'}_{\mathbf{k}}=-\frac{i}{\hbar}(\varepsilon_{c\mathbf{k}\mu}+\varepsilon_{v\mathbf{k}\mu'}-i\hbar\gamma-\hbar\nu_l)\sigma^{\mu\mu'}_{\mathbf{k}}$$

$$-i\sum_l g_{l\mathbf{k}\mu\mu'}(1-n^\mu_{e\mathbf{k}}-n^{\mu'}_{h-\mathbf{k}})A_{l\mu\mu'}$$

$$-\frac{i}{\hbar}\mu_B\mathbf{B}\cdot\left(\mathcal{G}_e\sum_\nu\mathbf{S}_{c\mu\nu}\sigma^{\nu\mu'}_{\mathbf{k}}+\mathcal{G}_h\sum_{\nu'}\mathbf{S}_{v\mu'\nu'}\sigma^{\mu\nu'}_{\mathbf{k}}\right)$$

$$+F^{\mu\mu'}_{\sigma_{\mathbf{k}}}\tag{6}$$

and

$$\frac{d}{dt}A_{l\mu\mu'}=\left[-\frac{\kappa^0_l}{2}+i(\nu_l-\Omega_l)\right]A_{l\mu\mu'}-i\sum_{\mathbf{k}}g^*_{l\mathbf{k}\mu\mu'}\sigma^{\mu\mu'}_{\mathbf{k}}$$

$$+F_l.\tag{7}$$

In these equations γ is the dipole dephasing rate and κ^0_l is the field decay rate, while $F^{\mu\mu'}_{\sigma_{\mathbf{k}}}$ and F_l are the fluctuation terms for the carriers and the field, respectively. In Eq. (7) Ω_l is the passive-cavity (active layer) frequency.[19]

Following Eq. (6) the magnetic field induces spin-flip between each subband. However, choosing conveniently the Faraday configuration (magnetic field orientated along the device, $\mathbf{B}=B_z\hat{\mathbf{k}}$) S_z involves only diagonal elements and the Eq. (6) is simplified to

$$\frac{d}{dt}\sigma^{\mu\mu'}_{\mathbf{k}}=-\frac{i}{\hbar}(\varepsilon_{c\mathbf{k}\mu}+\varepsilon_{v\mathbf{k}\mu'}-i\hbar\gamma-\hbar\nu_l)\sigma^{\mu\mu'}_{\mathbf{k}}$$

$$-i\sum_l g_{l\mathbf{k}\mu\mu'}(1-n^\mu_{e\mathbf{k}}-n^{\mu'}_{h-\mathbf{k}})A_{l\mu\mu'}$$

$$-\frac{i}{\hbar}\mu_B B_z(\mathcal{G}_e S^z_{c\mu\mu}\sigma^{\mu\mu'}_{\mathbf{k}}+\mathcal{G}_h S^z_{v\mu'\mu'}\sigma^{\mu\mu'}_{\mathbf{k}})$$

$$+F^{\mu\mu'}_{\sigma_{\mathbf{k}}},\tag{8}$$

and no spin flip is present.

Now considering the regime where the dipole dephasing rate is much smaller than the field decay rate, $\gamma\ll\kappa^0_l$ we can take the solution of Eq. (8) in the slow varying regime for the adiabatic approximation

$$\sigma^{\mu\mu'}_{\mathbf{k}}=\frac{i\sum_{l'}g_{l'\mathbf{k}\mu\mu'}(n^\mu_{e\mathbf{k}}+n^{\mu'}_{h-\mathbf{k}}-1)A_{l'\mu\mu'}+F^{\mu\mu'}_{\sigma_{\mathbf{k}}}}{\gamma+i[\mu_B B_z(\mathcal{G}_e S^z_{c\mu\mu}+\mathcal{G}_h S^z_{v\mu'\mu'})+\varepsilon_{c\mathbf{k}\mu}+\varepsilon_{v\mathbf{k}\mu'}-\hbar\nu_l)]/\hbar},\tag{9}$$

and substituting it into Eq. (7) we obtain for the photon annihilation operator

$$\frac{d}{dt}A_{l\mu\mu'}=[-\kappa_l^0/2+i(\nu_l-\Omega_l)]A_l+\sum_{l'}G_{ll'}^{\mu\mu'}A_{l'\mu\mu'}+F_{\sigma l}^{\mu\mu'}+F_l, \tag{10}$$

where the polarized gain matrix $G_{ll'}^{\mu\mu'}$ is defined as

with

$$G_{ll'}^{\mu\mu'}=\sum_{\mathbf{k}}G_{\mathbf{k}ll'}^{\mu\mu'}\equiv\sum_{\mathbf{k}}\mathcal{D}_{l\mathbf{k}\mu\mu'}g_{l\mathbf{k}\mu\mu'}^*g_{l'\mathbf{k}\mu\mu'}$$

$$\times(n_{e\mathbf{k}}^{\mu}+n_{h-\mathbf{k}}^{\mu'}-1), \tag{11}$$

and we defined a new fluctuation term

$$F_{\sigma l}^{\mu\mu'}\equiv-i\sum_{\mathbf{k}}g_{l\mathbf{k}\mu\mu'}^*\mathcal{D}_{l\mathbf{k}\mu\mu'}F_{\sigma_{\mathbf{k}}}^{\mu\mu'}, \tag{12}$$

$$\mathcal{D}_{l\mathbf{k}\mu\mu'}=\frac{1}{\gamma+i[\mu_BB_z(\mathcal{G}_eS_{c\mu\mu}^z+\mathcal{G}_hS_{v\mu'\mu'}^z)+\varepsilon_{c\mathbf{k}\mu}+\varepsilon_{v\mathbf{k}\mu'}-\hbar\nu_l]/\hbar}. \tag{13}$$

The photon number Langevin equation is obtained immediately from Eq. (10) and reads

$$\frac{d}{dt}n_{l\mu\mu'}=-\kappa_l^0n_{l\mu\mu'}+\sum_{l'}(G_{ll'}^{\mu\mu'}A_{l\mu\mu'}^{\dagger}A_{l'\mu\mu'}+\text{H.c.})$$

$$+\left[\left(\sum_{\mu\mu'}F_{\sigma l}^{\mu\mu'}+F_l\right)A_{l\mu\mu'}^{\dagger}+\text{H.c.}\right]. \tag{14}$$

Equation (14) explicitly shows the polarizations μ and μ' dependence, while the dissipative term is independent of polarization once $\kappa_l^0=\nu_l/Q$, where Q is the cavity (active layer) quality factor.

Correlations between distinct modes can be important, as for example in the generation of sub-Poissonian light,[21,22] however, for our interest here, we consider the simple situation when correlations between distinct modes can be neglected, and thus

$$\langle A_{l\mu\mu'}^{\dagger}(t)A_{l'\rho\rho'}(t)\rangle=\langle n_l\rangle\delta_{ll'}\delta_{\mu\rho}\delta_{\mu'\rho'}, \tag{15}$$

$$\langle\sigma_{\mathbf{k}}^{\dagger\mu\mu'}(t)\sigma_{\mathbf{k}'}^{\rho\rho'}(t)\rangle=\langle n_{e\mathbf{k}}^{\mu}n_{h-\mathbf{k}}^{\mu'}\rangle\delta_{ll'}\delta_{\mu\rho}\delta_{\mu'\rho'}, \tag{16}$$

$$\langle\sigma_{\mathbf{k}}^{\mu\mu'}(t)\sigma_{\mathbf{k}}^{\dagger\rho\rho'}(t)\rangle=\langle(1-n_{e\mathbf{k}}^{\mu})(1-n_{h-\mathbf{k}}^{\mu'})\rangle\delta_{ll'}\delta_{\mu\rho}\delta_{\mu'\rho'}, \tag{17}$$

$$\langle n_{e\mathbf{k}}^{\mu}(t)n_{e\mathbf{k}'}^{\rho}(t)\rangle=\langle n_{e\mathbf{k}}^{\mu}\rangle\delta_{\mathbf{k}\cdot\mathbf{k}'}\delta_{\mu\rho}, \tag{18}$$

$$\langle F_{\sigma_{\mathbf{k}}}^{\dagger\mu\mu'}(t)F_{\sigma_{\mathbf{k}}'}^{\rho\rho'}(t)\rangle=2D_{\sigma_{\mathbf{k}}^{\dagger}\sigma_{\mathbf{k}'}}^{\mu\mu'}\delta(t-t')\delta_{\mu\rho}\delta_{\mu'\rho'}\delta_{\mathbf{k}\cdot\mathbf{k}'}. \tag{19}$$

To determine the fluctuation terms we have to recall the generalized Einstein relation.[19] If the generalized Langevin equation is given by

$$\frac{d}{dt}A_{\mu}=D_{\mu}+F_{\mu} \tag{20}$$

then the generalized Einstein relation will be

$$2D_{\mu\nu}=\frac{d}{dt}\langle A_{\mu}A_{\nu}\rangle-\langle D_{\mu}A_{\nu}\rangle-\langle A_{\mu}D_{\nu}\rangle \tag{21}$$

and

$$\langle F_{\mu}(t)F_{\nu}(t')\rangle=2D_{\mu\nu}\delta(t-t'), \tag{22}$$

which is a manifestation of the fluctuation-dissipation theorem.[26]

Referring back to the Eq. (8) we find the following diffusion term:

$$2D_{\sigma_{\mathbf{k}}^{\dagger}\sigma_{\mathbf{k}'}}^{\mu\mu'}=\frac{d}{dt}\langle\sigma_{\mathbf{k}}^{\dagger\mu\mu'}\sigma_{\mathbf{k}'}^{\rho\rho'}\rangle+2\gamma\langle\sigma_{\mathbf{k}}^{\dagger\mu\mu'}\sigma_{\mathbf{k}'}^{\rho\rho'}\rangle=\frac{d}{dt}\langle n_{e\mathbf{k}}^{\mu}n_{h-\mathbf{k}}^{\mu'}\rangle$$

$$+2\gamma\langle n_{e\mathbf{k}}^{\mu}n_{h-\mathbf{k}}^{\mu'}\rangle. \tag{23}$$

Assuming the quasiequilibrium condition

$$\frac{d}{dt}\langle n_{e\mathbf{k}}^{\mu}n_{h-\mathbf{k}}^{\mu'}\rangle\ll2\gamma\langle n_{e\mathbf{k}}^{\mu}n_{h-\mathbf{k}}^{\mu'}\rangle, \tag{24}$$

we obtain

$$\langle F_{\sigma_{\mathbf{k}}}^{\dagger\mu\mu'}(t)F_{\sigma_{\mathbf{k}}'}^{\rho\rho'}(t)\rangle=2\gamma\langle n_{e\mathbf{k}}^{\mu}n_{h-\mathbf{k}}^{\mu'}\rangle\delta(t-t')\delta_{\mu\rho}\delta_{\mu'\rho'}\delta_{\mathbf{k}\cdot\mathbf{k}'}. \tag{25}$$

Analogously

$$\langle F_{\sigma_{\mathbf{k}}}^{\mu\mu'}(t)F_{\sigma_{\mathbf{k}}'}^{\dagger\rho\rho'}(t)\rangle=2\gamma\langle(1-n_{e\mathbf{k}}^{\mu})(1-n_{h-\mathbf{k}}^{\mu'})\rangle$$

$$\times\delta(t-t')\delta_{\mu\rho}\delta_{\mu'\rho'}\delta_{\mathbf{k}\cdot\mathbf{k}'}. \tag{26}$$

For the light-field Langevin-force, considering the non-correlation between modes, as is well known[19]

$$\langle F_l^\dagger(t)F_{l'}(t')\rangle = \kappa_l^0 \bar{n}_0(\nu_l)\delta(t-t')\delta_{ll'}, \qquad (27)$$

where $\bar{n}_0(\nu_l)$ is the number of thermal photons. For the carriers Langevin force, we obtain the time correlation

$$\langle F_{\sigma l}^{\dagger \mu\mu'}(t)F_{\sigma l}^{\rho\rho'}(t')\rangle = \sum_{\mathbf{k}k'} g_{l\mathbf{k}\mu\mu'}^* g_{l\mathbf{k}'\mu\mu'}\mathcal{D}_{l\mathbf{k}\mu\mu'}^* \mathcal{D}_{l\mathbf{k}'\mu\mu'}$$

$$\times \langle F_{\sigma_\mathbf{k}}^{\dagger \mu\mu'}(t)F_{\sigma_\mathbf{k}}^{\mu\mu'}(t')\rangle$$

$$= \sum_{\mathbf{k}k'} g_{l\mathbf{k}\mu\mu'}^* g_{l\mathbf{k}'\mu\mu'}\mathcal{D}_{l\mathbf{k}\mu\mu'}^* \mathcal{D}_{l\mathbf{k}'\mu\mu'}2\gamma$$

$$\times \langle n_{e\mathbf{k}}^\mu(t)n_{h-\mathbf{k}}^{\mu'}\rangle\delta(t-t')\delta_{\mu\rho}\delta_{\mu'\rho'}\delta_{\mathbf{k}\cdot\mathbf{k}'}$$

$$= \sum_{\mathbf{k}} |g_{l\mathbf{k}\mu\mu'}|^2|\mathcal{D}_{l\mathbf{k}\mu\mu'}|^2 2\gamma\langle n_{e\mathbf{k}}^\mu(t)n_{h-\mathbf{k}}^{\mu'}\rangle$$

$$\times \delta(t-t')\delta_{\mu\rho}\delta_{\mu'\rho'}. \qquad (28)$$

Rewriting it in terms of the Lorentzian line shape $\mathcal{L}_{l\mathbf{k}}^{\mu\mu'} \equiv \gamma^2|\mathcal{D}_{l\mathbf{k}\mu\mu'}|^2$, and the spontaneous emission rate into the mode l due to the transition $\mu\mu'$, $R_{sp,l}^{\mu\mu'}$, given by

$$R_{sp,l}^{\mu\mu'} \equiv \frac{2}{\gamma}\sum_{\mathbf{k}} |g_{l\mathbf{k}\mu\mu'}|^2\mathcal{L}_{l\mathbf{k}}^{\mu\mu'}n_{e\mathbf{k}}^\mu n_{h-\mathbf{k}}^{\mu'}, \qquad (29)$$

we get

$$\langle F_{\sigma l}^{\dagger \mu\mu'}(t)F_{\sigma l}^{\rho\rho'}(t')\rangle = \langle R_{sp,l}^{\mu\mu'}\rangle\delta(t-t')\delta_{\mu\rho}\delta_{\mu'\rho'}. \qquad (30)$$

Similarly

$$\langle F_{\sigma l}^{\mu\mu'}(t)F_{\sigma l}^{\dagger\rho\rho'}(t')\rangle = \langle R_{abs,l}^{\mu\mu'}\rangle\delta(t-t')\delta_{\mu\rho}\delta_{\mu'\rho'}, \qquad (31)$$

where the absorption rate is defined as

$$R_{abs,l}^{\mu\mu'} \equiv \frac{2}{\gamma}\sum_{\mathbf{k}} |g_{l\mathbf{k}\mu\mu'}|^2\mathcal{L}_{l\mathbf{k}}^{\mu\mu'}(1-n_{e\mathbf{k}}^\mu)(1-n_{h-\mathbf{k}}^{\mu'}). \qquad (32)$$

Neglecting $l\neq l'$ (intermode) correlations the photon-number Langevin equation is then written as

$$\frac{d}{dt}n_{l\mu\mu'} = -\kappa_l^0 n_{l\mu\mu'} + (G_{ll}^{\mu\mu'}+G_{ll}^{*\mu\mu'})n_{l\mu\mu'}$$

$$+ [(F_{\sigma l}^{\mu\mu'}+F_l)A_{l\mu\mu'}^\dagger + \text{H.c.}], \qquad (33)$$

and noticing that

$$G_{ll}^{\mu\mu'}+G_{ll}^{*\mu\mu'} = R_{sp,l}^{\mu\mu'}-R_{abs,l}^{\mu\mu'}, \qquad (34)$$

then

$$\frac{d}{dt}n_{l\mu\mu'} = -\kappa_l^0 n_{l\mu\mu'} - (R_{abs,l}^{\mu\mu'}-R_{sp,l}^{\mu\mu'})n_{l\mu\mu'}$$

$$+ [(F_{\sigma l}^{\mu\mu'}+F_l)A_{l\mu\mu'}^\dagger + \text{H.c.}]. \qquad (35)$$

The steady state solution of Eq. (35) is readily obtained, to give the steady average photon number in the mode l

$$\bar{n}_{l\mu\mu'} = \frac{\langle(F_{\sigma l}^{\mu\mu'}A_{l\mu\mu'}^\dagger + \text{H.c.})\rangle + \langle(F_l A_{l\mu\mu'}^\dagger + \text{H.c.})\rangle}{\kappa_l^0 + (\langle R_{abs,l}^{\mu\mu'}\rangle - \langle R_{sp,l}^{\mu\mu'}\rangle)}. \qquad (36)$$

To calculate the correlations $\langle F_{\sigma l}^{\mu\mu'}(t)A_{l\mu\mu'}^\dagger(t)\rangle$ and $\langle F_l(t)A_{l\mu\mu'}^\dagger(t)\rangle$ we assume that

$$A_{l\mu\mu'}(t) = A_{l\mu\mu'}(t-\Delta t) + \int_{t-\Delta t}^t dt'\dot{A}_{l\mu\mu'}(t'), \qquad (37)$$

where Δt is an interval much shorter than $1/\kappa_l^0$ but much longer than the correlation time of the field reservoir.[19] Substituting Eq. (10) into (37) we can calculate the above correlations, which then are given by

$$\langle F_l(t)A_{l\mu\mu'}^\dagger(t) + \text{H.c.}\rangle = \kappa_l^0 \bar{n}_0(\nu_l), \qquad (38)$$

$$\langle F_{\sigma l}^{\mu\mu'}(t)A_{l\mu\mu'}^\dagger(t) + \text{H.c.}\rangle = \langle R_{sp,l}^{\mu\mu'}\rangle. \qquad (39)$$

Substituting these correlations into Eq. (36) we finally obtain

$$\bar{n}_{l\mu\mu'} = \frac{\kappa_l^0 \bar{n}_0(\nu_l) + \langle R_{sp,l}^{\mu\mu'}\rangle}{\kappa_l^0 + (\langle R_{abs,l}^{\mu\mu'}\rangle - \langle R_{sp,l}^{\mu\mu'}\rangle)}, \qquad (40)$$

which shows exactly how the absorption and emission rate contribute to the steady average photon number in mode l. As it is expected, $\bar{n}_0(\nu_l)$ coming from a thermal reservoir (thermal photons) does not contribute to a specific polarization. In the device working regime $\langle R_{sp,l}^{\mu\mu'}\rangle \gg \kappa_l^0\bar{n}_0(\nu_l)$, the radiative recombination process determines the light polarization. However, the increase of temperature may blur the light polarization. We further analyze this point in the next section for the measurement of the polarized light.

IV. MEASUREMENT OF SPIN POLARIZATION BY DETECTION OF EMITTED LIGHT

At this point it is interesting to analyze the degree of polarization of the emitted light as a function of the carriers recombination. For that we will focus on the l-mode photon flux N_l at the photodetector (see Fig. 1), which we assume as placed at the wall of the semiconductor active layer "microcavity."[20] The input-output theory[20,24,31] determines that the relation between the output, input and the cavity field is given by

$$V_l^{\mu\mu'} = \kappa_l^0 n_{l\mu\mu'} - F_{\kappa,l}, \qquad (41)$$

where $V_l^{\mu\mu'}$ is the photon flux of mode l from the cavity (active layer of the LED) and $F_{\kappa,l}$ is the input field fluctuation, which in our case is a thermal white noise. Now the relation between the emitted flux $V_l^{\mu\mu'}$ and the detected flux $\bar{N}_l^{\mu\mu'}$ is given by

$$\bar{N}_l^{\mu\mu'} = \xi_l\langle V_l^{\mu\mu'}\rangle, \qquad (42)$$

where $\xi_l \equiv \xi(\nu_l)$ is the transmission coefficient of mode l. ξ_l is related to the spectral response of the photodetector. A nonhomogeneous-detection process reflects a structured response due to a narrow-band photodetector. In the case of homogeneous detection, or a broad-band detector, $\xi_l = \beta_0$ is a flat distribution over the frequencies.[32] We shall consider only this last situation. Thus the total detected photon number is $\bar{N}^{\mu\mu'} = \Sigma_l \bar{N}_l^{\mu\mu'} = \beta_0 \Sigma \langle V_l^{\mu\mu'} \rangle$. Since we did not consider correlations between modes, the total detected photon number is a summation of the photon number of each mode. Therefore, from now on it is enough to consider the calculations for one mode only the extension for the multimodes being a simple exercise. The electroluminescence intensity in right (σ^+) and left (σ^-) circular polarization are given by $\bar{N}_l^+ = \bar{N}_l^{-1/2 - 3/2} + \bar{N}_l^{1/2 - 1/2}$ and $\bar{N}_l^- = \bar{N}_l^{-1/2(1/2)} + \bar{N}_l^{1/2(3/2)}$, respectively. We simplify our treatment if we consider the low injection limit $\kappa_l^0 \gg \langle R_{\mathrm{abs},l}^{\mu\mu'} - R_{\mathrm{sp},l}^{\mu\mu'} \rangle$, where we can rewrite Eq. (40) simply as

$$\bar{n}_{l\mu\mu'} = \bar{n}_0(\nu_l) + \langle R_{\mathrm{sp},l}^{\mu\mu'} / \kappa_l^0 \rangle, \qquad (43)$$

and so, the photon flux at the detector is

$$\bar{N}_l^{\mu\mu'} = \beta_0 [\kappa_l^0 \bar{n}_0(\nu_l) + R_{\mathrm{sp},l}^{\mu\mu'}]. \qquad (44)$$

Following Ref. 13 the spectral degree of polarization of the detected light in mode l is given by

$$\mathcal{P}(\nu_l) = \frac{\bar{I}^+ - \bar{I}^-}{\bar{I}^+ + \bar{I}^-}, \qquad (45)$$

where $I^{\pm} \equiv N_l^{\pm}/\xi_l$, is the light intensity at the detector. Substituting Eqs. (41) and (42) into Eq. (45) for a broad band detector, we obtain the spectral degree of polarization in terms of the average photon-number in mode l

$$\mathcal{P}(\nu_l) = \frac{\bar{n}_{l-1/2-3/2} + \bar{n}_{l1/2-1/2} - \bar{n}_{l-1/2(1/2)} - \bar{n}_{l1/2(3/2)}}{\bar{n}_{l-1/2-3/2} + \bar{n}_{l1/2-1/2} + \bar{n}_{l-1/2(1/2)} + \bar{n}_{l1/2(3/2)}} \qquad (46)$$

which is independent of the transmission efficiency β_0. In the low injection limit $\kappa_l^0 \gg \langle R_{\mathrm{abs},l}^{\mu\mu'} - R_{\mathrm{sp},l}^{\mu\mu'} \rangle$, Eq. (46) writes

$$\mathcal{P}(\nu_l) = \frac{\langle R_{\mathrm{sp},l}^{-1/2-3/2} + R_{\mathrm{sp},l}^{1/2-1/2} - R_{\mathrm{sp},l}^{-1/2(1/2)} - R_{\mathrm{sp},l}^{1/2(3/2)} \rangle}{\langle R_{\mathrm{sp},l}^{-1/2-3/2} + R_{\mathrm{sp},l}^{1/2-1/2} + R_{\mathrm{sp},l}^{-1/2(1/2)} + R_{\mathrm{sp},l}^{1/2(3/2)} \rangle + 4\kappa_l^0 \bar{n}_0(\nu_l)}. \qquad (47)$$

The role of the material dipole matrix for the degree of polarization is made clear trough the spontaneous emission rate $R_{\mathrm{sp},l}^{\mu\mu'}$ from Eq. (29), as well as the polarization dependence on the thermal photon number. Notice that the broader is the detector spectral response the stronger will be the counter effect of thermal photons over the intrinsic degree of polar-

ization. For a sufficiently broad spectral response, as the temperature is raised the unpolarized thermal photons become more and more important in the process, decreasing the degree of polarization of the emitted light.

V. INTRINSIC POLARIZATION

Let us focus our discussion on the analysis of the intrinsic polarization of the GaAs electroluminescence spectra as a function of the temperature and the applied magnetic field. In Fig. 3 we plot the electroluminescence spectra with right and left circular polarization, for several magnetic fields (0, 1, 4, and 8 T) with the temperature set to $T = 4.2$ K. To estimate it quantitatively we have assumed that the dipole matrix elements are given by the $\mathbf{k} \cdot \mathbf{p}$ theory in the parabolic band model, being
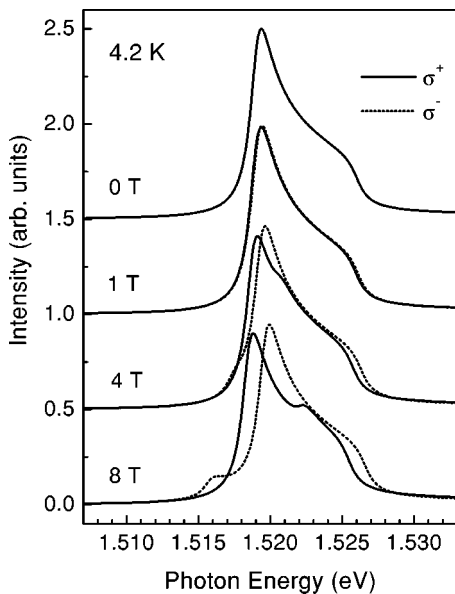
$$g_{\mathbf{k}l\mu\mu'} = g_{l\mu\mu'}(0) \frac{\varepsilon_g}{\varepsilon_g + \dfrac{\hbar^2 k^2}{2}\left(\dfrac{1}{m_\mu} + \dfrac{1}{m_{\mu'}}\right)}, \qquad (48)$$

where

$$g_{l\mu\mu'}(0) = \frac{ie p_{\mu\mu'}}{m_0 \varepsilon_g} \qquad (49)$$

FIG. 3. Intrinsic electroluminescence spectra of GaAs as function of the magnetic field.
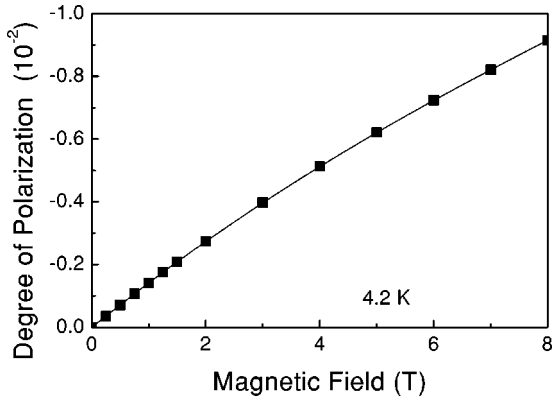
FIG. 4. Intrinsic degree of polarization of GaAs in function of the magnetic field.

is the dipole momentum at the center of the band, with e for the electron charge, and $p_{\mu\mu'}$ for the electron momentum given by the selection rules. All parameters are set to match optical transitions in GaAs.

From Fig. 3 we observe that this simple parabolic band model is reasonably good enough to give a qualitative picture of the spectra of the polarized light emission, including light-hole and heavy-hole features.[14] In Fig. 3 the solid line stands for right-circular polarization emission, while the dotted line stands for left-circular polarization emission. At $B = 0$ T there is no light polarization and both components have the same line shape. As the magnetic field is increased a slight splitting of both spectra are noticeable and at 8 T they can be completely distinguished. We have observed from our calculations that the strongest contribution for the deformation of the polarized-light spectra is due to the heavy-hole feature, as it is expected.[11,13] Notice that some of the spectral features have opposite polarization, reducing thus the net light emission polarization as confirmed experimentally by Jonker *et al.*[14] Those line shapes can be strongly modified by the variation of the width of the GaAs quantum well in the AlGaAs/GaAs/AlGaAs LED, which mainly affects the energy splitting of the heavy- and light-hole bands.

The intrinsic degree of polarization of the GaAs is given by integrating Eq. (47) over the frequency range P
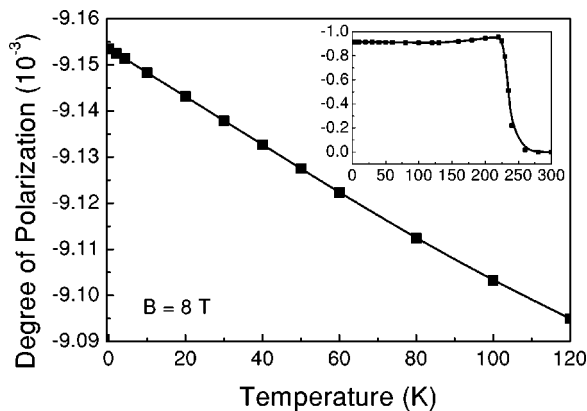

FIG. 5. Decreasing of intrinsic polarization of GaAs as a function of the temperature.

$= \int d\nu_l \mathcal{P}(\nu_l)$. In Fig. 4 we plot the GaAs intrinsic degree of polarization varying the magnetic field with the temperature set to 4.2 K. Figure 4 shows an almost linear behavior of the degree of polarization for a weak magnetic field $B \lesssim 1$ T. However, as the magnetic field is increased the polarization attains a polynomial shape. The calculated intrinsic polarization for carrier radiative recombination corroborates qualitatively with the experimentally measured photoluminescence intrinsic degree of polarization for GaAs given in Ref. 11 and quantitatively for electroluminescence measurements given in Ref. 33.

The variation of the intrinsic polarization with the temperature is plotted in Fig. 5 for a magnetic field set to 8 T. The temperature dependence of the electronic g factor is the main responsible by the slightly decrease of the degree of polarization shown in the figure, once the GaAs electronic g factor decreases with the temperature as $\mathcal{G}_e = -0.44 + 5 \times 10^{-4} T$,[18] turning the conduction band spin-splitting less sensitive to the magnetic field. Within our model a threshold for the decrease of the polarization is observed around $T_c = 235$ K, where T_c is a critical temperature dependent on the spectral response range of the light detector. For the present calculation we have fixed the detector frequency range to 1 eV, which is a reasonably good range for detection of the central carrier radiative recombination features. The threshold is due to thermal photons emission. At higher temperatures thermal photons are largely emitted, washing out the polarized emission around 1.519 eV and the intrinsic degree of polarization decreases abruptly as in the inset of Fig. 5. The slight increase of the polarization before the threshold at T_c is due to the fact that thermal photons start to contribute at lower frequencies from the left side of the emission spectra (Fig. 3) washing out first the central peak feature polarization and then only a right-lateral feature contribution enters into the computation of the degree of polarization. The dependence of the critical temperature with the detector spectral response is an interesting issue, and is going to be addressed elsewhere. Anyhow, in addition to the well known mechanisms preventing efficient spin injection at room temperature (see, e.g., Ref. 33), the observation of spin polarized carrier injection by means of optical polarization is also highly inefficient at those temperatures, since thermal photons emission reduces the net optical polarization.[34] We note that even the 2% efficiency of spin polarized carrier injection at room temperature observed by optical means in Ref. 33 was calculated by considering only lateral features of the emission spectrum. Indeed, the net polarization calculated by considering their whole spectrum is drastically reduced to approximately zero, in complete agreement with our calculations (inset of Fig. 5).

VI. CARRIER PUMPING AND NONRADIATIVE RECOMBINATION

A. Carrier Langevin equation and light emission polarization rate

It is interesting to analyze the problem of polarized electroluminescence if an unbalanced carrier injection is taken into account. In such a nonequilibrium case, fluctuation ef-

fects of carrier pumping and recombination are very important. For that we also write a Langevin equation for the electron number operator including carrier pumping, nonradiative recombination and dissipative effects as well. In light emitting devices, contrarily to laser diodes, there is very little optical feedback (if any), and so stimulated emission and absorption can be neglected.[22] Nonradiative recombination is introduced phenomenologically, following Refs. 19,20. The Langevin equation for the carrier occupation probability can be written as

$$
\frac{d}{dt} n_{e\mathbf{k}}^{\mu} = \Lambda_{e\mathbf{k}}^{\mu}(1 - n_{e\mathbf{k}}^{\mu}) - \gamma_{NR}^{\mu} n_{e\mathbf{k}}^{\mu} + \sum_{l\mu'} (ig_{l\mathbf{k}\mu\mu'}^{*} A_{l\mu\mu'}^{\dagger} \sigma_{\mathbf{k}}^{\mu\mu'}
$$
$$
+ \text{H.c.}) + F_{e\mathbf{k}}^{\mu},
\tag{50}
$$

where $\Lambda_{e\mathbf{k}}^{\mu}$ is the pumping rate due to a current injection, $(1 - n_{e\mathbf{k}}^{\mu})$ is the pump blocking, γ_{NR}^{μ} is the nonradiative recombination parameter included phenomenologically, and $F_{e\mathbf{k}}^{\mu}$ is the μ-polarized electron number fluctuation term.

Using again the quasiequilibrium condition (9), we obtain

$$
\frac{d}{dt} n_{e\mathbf{k}}^{\mu} = \Lambda_{e\mathbf{k}}^{\mu}(1 - n_{e\mathbf{k}}^{\mu}) - \gamma_{NR}^{\mu} n_{e\mathbf{k}}^{\mu}
$$
$$
- \sum_{ll'\mu'} [\mathcal{D}_{l\mathbf{k}\mu\mu'} g_{l\mathbf{k}\mu\mu'} g_{l'\mathbf{k}\mu\mu'}^{*} A_{l\mu\mu'}^{\dagger} A_{l'\mu\mu'}
$$
$$
\times (n_{e\mathbf{k}}^{\mu} + n_{h-\mathbf{k}}^{\mu'} - 1) + \text{H.c.}]
$$
$$
+ \sum_{l\mu'} (i\mathcal{D}_{l\mathbf{k}\mu\mu'} g_{l\mathbf{k}\mu\mu'}^{*} A_{l\mu\mu'}^{\dagger} F_{\sigma_{\mathbf{k}}}^{\mu\mu'} + \text{H.c.}) + F_{e\mathbf{k}}^{\mu}.
\tag{51}
$$

This last equation can be further simplified by neglecting correlation between modes, such that

$$
\frac{d}{dt} n_{e\mathbf{k}}^{\mu} = \Lambda_{e\mathbf{k}}^{\mu}(1 - n_{e\mathbf{k}}^{\mu}) - \gamma_{NR}^{\mu} n_{e\mathbf{k}}^{\mu} - \sum_{l\mu'} (G_{\mathbf{k}ll}^{\mu\mu'} + G_{\mathbf{k}ll}^{*\mu\mu'}) n_{l\mu\mu'}
$$
$$
+ \sum_{l\mu'} (i\mathcal{D}_{l\mathbf{k}\mu\mu'} g_{l\mathbf{k}\mu\mu'}^{*} A_{l\mu\mu'}^{\dagger} F_{\sigma_{\mathbf{k}}}^{\mu\mu'} + \text{H.c.}) + F_{e\mathbf{k}}^{\mu}.
\tag{52}
$$

Since the third term of the right-hand side of Eq. (52) is due to the radiative recombination we can simplify it by just relating it to the radiative decay rate as follows:[19,23]

$$
\frac{d}{dt} n_{e\mathbf{k}}^{\mu} = \Lambda_{e\mathbf{k}}^{\mu}(1 - n_{e\mathbf{k}}^{\mu}) - \gamma_{NR}^{\mu} n_{e\mathbf{k}}^{\mu} - \gamma_{r}^{\mu} n_{e\mathbf{k}}^{\mu} + F_{e\mathbf{k}}^{\mu}, \tag{53}
$$

where we have also included the fourth term of Eq. (52) in the definition of $F_{e\mathbf{k}}^{\mu}$, and obviously, γ_{r}^{μ} is a carrier occupation number dependent function as

$$
\gamma_{r}^{\mu} = \frac{\sum_{l\mu'} (G_{\mathbf{k}ll}^{\mu\mu'} + G_{\mathbf{k}ll}^{*\mu\mu'}) n_{l\mu\mu'}}{n_{e\mathbf{k}}^{\mu}}
\tag{54}
$$

and $G_{\mathbf{k}ll}^{\mu\mu'}$ is also an implicit function of $n_{e\mathbf{k}}^{\mu}$. Depending on the process involved in the nonradiative recombination, γ_{NR}^{μ} can also be $n_{e\mathbf{k}}^{\mu}$ dependent. For simplicity we have taken both the radiative and nonradiative recombination rates as constants, and as such independent of the magnetic field. In this regime the average value for the carrier number is given as a function of the pumping rate as

$$
\langle n_{e\mathbf{k}}^{\mu}(t) \rangle = \left(\langle n_{e\mathbf{k}}^{\mu}(0) \rangle - \frac{\Lambda_{e\mathbf{k}}^{\mu}}{\Lambda_{e\mathbf{k}}^{\mu} + \gamma_{NR}^{\mu} + \gamma_{r}^{\mu}} \right) e^{-(\Lambda_{e\mathbf{k}}^{\mu} + \gamma_{NR}^{\mu} + \gamma_{r}^{\mu})t}
$$
$$
+ \frac{\Lambda_{e\mathbf{k}}^{\mu}}{\Lambda_{e\mathbf{k}}^{\mu} + \gamma_{NR}^{\mu} + \gamma_{r}^{\mu}},
\tag{55}
$$

whose stationary solution is

$$
\langle n_{e\mathbf{k}}^{\mu} \rangle_{\text{eq}} = \frac{\Lambda_{e\mathbf{k}}^{\mu}}{\Lambda_{e\mathbf{k}}^{\mu} + \gamma_{NR}^{\mu} + \gamma_{r}^{\mu}}.
\tag{56}
$$

Similarly the equilibrium hole occupation probability is given by

$$
\langle n_{h-\mathbf{k}}^{\mu'} \rangle_{\text{eq}} = \frac{\Lambda_{h-\mathbf{k}}^{\mu'}}{\Lambda_{h-\mathbf{k}}^{\mu'} + \gamma_{NR}^{\mu'} + \gamma_{r}^{\mu'}},
\tag{57}
$$

where $\Lambda_{h-\mathbf{k}}^{\mu'}$ is the hole pumping rate and $\gamma_{NR}^{\mu'}$ and $\gamma_{r}^{\mu'}$ are the nonradiative and radiative hole recombination rate, respectively. Thus the expected spontaneous emission rate (29) can be simply given by

$$
\langle R_{\text{sp},l}^{\mu\mu'} \rangle = \frac{\gamma}{2} \sum_{\mathbf{k}} |g_{l\mathbf{k}\mu\mu'}|^{2}
$$
$$
\times \mathcal{L}_{l\mathbf{k}}^{\mu\mu'} \frac{\Lambda_{e\mathbf{k}}^{\mu} \Lambda_{h-\mathbf{k}}^{\mu'}}{(\Lambda_{e\mathbf{k}}^{\mu} + \gamma_{NR}^{\mu} + \gamma_{r}^{\mu})(\Lambda_{h-\mathbf{k}}^{\mu'} + \gamma_{NR}^{\mu'} + \gamma_{r}^{\mu'})}.
\tag{58}
$$

To use this last expression, it is convenient to write the spectral light polarization as given by Eq. (47) in the following compact form:

$$
\mathcal{P}(\nu_{l}) = \frac{\sum_{\mu\mu'} (\mu - \mu') \langle R_{\text{sp},l}^{\mu\mu'} \rangle}{\left[\sum_{\mu\mu'} \langle R_{\text{sp},l}^{\mu\mu'} \rangle + 4\bar{n}_{0}(\nu_{l}) \right]},
\tag{59}
$$

where we must remember that the elements $R_{\text{sp},l}^{-1/2 - 1/2} = R_{\text{sp},l}^{-1/2(3/2)} = R_{\text{sp},l}^{1/2 - 3/2} = R_{\text{sp},l}^{1/2(1/2)} = 0$. Substituting Eq. (58) into Eq. (59) the spectral light polarization is finally given in function of the balance of electron and hole injection as

$$
\mathcal{P}(\nu_{l}) = \frac{\sum_{\mathbf{k}\mu\mu'} (\mu - \mu') |g_{l\mathbf{k}\mu\mu'}|^{2} \mathcal{L}_{l\mathbf{k}}^{\mu\mu'} \Gamma_{\mathbf{k}}^{\mu\mu'}}{\left[\sum_{\mathbf{k}\mu\mu'} \left| g_{l\mathbf{k}\mu\mu'} \right|^{2} \mathcal{L}_{l\mathbf{k}}^{\mu\mu'} \Gamma_{\mathbf{k}}^{\mu\mu'} + 8\bar{n}_{0}(\nu_{l})/\gamma \right]},
\tag{60}
$$

where we have defined

$$\Gamma_{\mathbf{k}}^{\mu\mu'} \equiv \frac{\Lambda_{e\mathbf{k}}^{\mu}\Lambda_{h-\mathbf{k}}^{\mu'}}{(\Lambda_{e\mathbf{k}}^{\mu} + \gamma_{NR}^{\mu} + \gamma_{r}^{\mu})(\Lambda_{h-\mathbf{k}}^{\mu'} + \gamma_{NR}^{\mu'} + \gamma_{r}^{\mu'})}, \qquad (61)$$

as the pumping to recombination rate. As before the light degree of polarization is given by integrating Eq. (60).

B. Pumping rate modeling

Before proceed further we need to discuss the phenomenologically introduced pumping rate in detail. When summing over $\mathbf{k}$ the pumping and pump blocking term for the α carrier ($\alpha = e$, or h), must be related to the spin polarized current density J_{μ} (Refs. 19,23) by

$$\sum_{\mathbf{k}} \Lambda_{\alpha\mathbf{k}}^{\mu}(1 - n_{e\mathbf{k}}^{\mu}) = \frac{\eta J_{\mu}}{ed}, \qquad (62)$$

where η is the total quantum efficiency that the injected carriers contribute to the population of the $\alpha\mu$ subband, e is the electron charge, and d is the thickness of the active region. Assuming that by the time the injected carriers reach the active region they collide often enough to be in equilibrium within each subband, it is reasonable to assume the quasiequilibrium condition[19,23] such that

$$\Lambda_{\alpha\mathbf{k}}^{\mu} = \frac{\eta_{tr}J_{\mu}}{edN_0}f_{\alpha\mathbf{k}0}, \qquad (63)$$

where N_0 and $f_{\alpha\mathbf{k}0}$ are the total carriers density and the Fermi-Dirac distribution function, respectively, at zero bias. η_{tr} is the transport part of the quantum efficiency, giving the efficiency that the injected carriers reach the active region. η_{tr} could include a spinorial dependence to take into account dephasing and decoherence mechanisms at the spin-aligner material and GaAs interface.[30] However, such mechanisms are not concerned in the present work. The spin dependent current density J_{μ} is related to the spin-alignment efficiency of the material cap layer (Fig. 1). Spin-aligner materials such as $Be_{1-x-y}Mn_xZn_ySe$,[11] $Zn_{1-x}Mn_xSe$,[13] or ferromagnetic GaMnAs epilayers[12] show giant magnetoresistance.[27,28] Thus J_{μ} must take into account the magnetic field strength relating spin aligned carrier injection into the GaAs LED. From Refs. 11–14,33 the spin aligned current injection follows closely the profile of a Brillouin paramagnet, whose net magnetization is phenomenologically given by[27]

$$M = \frac{\bar{x}}{x}\mathcal{G}_{\alpha}'\mu_B S\mathcal{B}_S\left(\frac{\mathcal{G}_{\alpha}'\mu_B SB}{k_B(T+T_0)}\right), \qquad (64)$$

where $\mathcal{G}_{\alpha}'$ is the magnetic material electronic g factor, S is the magnetic material spin, $\mathcal{B}_S$ is a S-Brillouin function, and $\bar{x}/x$ is the molar fraction of Mn contributing to the saturation of the magnetization and T_0 is a fitting temperature to scale with the experimental magnetization curve.[27] Since the degree of polarization of the injected current is directly proportional to the magnetization and also directly proportional to the magnetic semiconductor layer thickness d_{MS}, we assume the following phenomenological electronic injection current density:
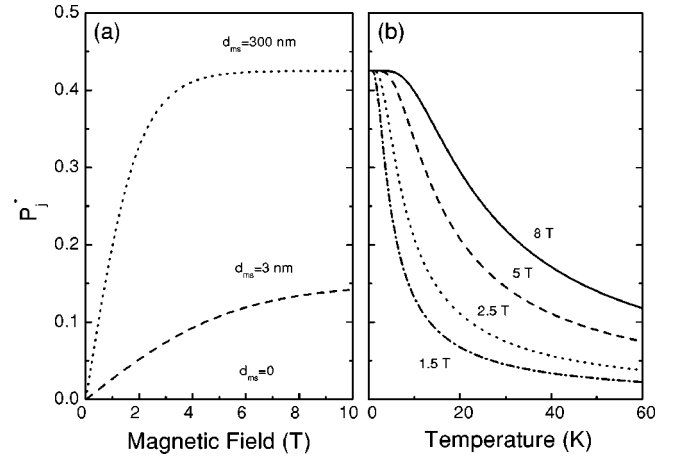

FIG. 6. Normalized polarization of injected carriers into LED from a Brillouin magnetic semiconductor. (a) Carrier injection polarization dependence with the applied magnetic field and magnetic semiconductor thickness d_{MS} at $T = 4.2$ K. (b) Carrier injection polarization dependence with the temperature for $d_{MS} = 300$ nm.

$$J_{\mu} = \frac{J_0}{2} + d_{MS}\frac{\bar{x}}{x}\mathcal{G}_e'\mu_B\mu\mathcal{B}_{1/2}\left(\frac{\mathcal{G}_e'\mu_B B d_{MS}}{2k_B T d_0}\right), \qquad (65)$$

where J_0 is the net current density without a magnetic field. The net current is always J_0, but each component of J_{μ} is increased or decreased if $\mu = 1/2$ or $-1/2$, respectively. Remark that instead of T_0 we included the fraction d_{MS}/d_0 as a fitting parameter, where d_0 is a fitting length, which is more convenient for our purposes. If we define the polarization of the injected current by

$$P_j \equiv \frac{J_{1/2} - J_{-1/2}}{J_{1/2} + J_{-1/2}}, \qquad (66)$$

which is the rate between spin and charge current densities, we obtain by Eq. (65)

$$P_j = \frac{1}{J_0}d_{MS}\frac{\bar{x}}{x}\mathcal{G}_e'\mu_B\mathcal{B}_{1/2}\left(\frac{\mathcal{G}_e'\mu_B B d_{MS}}{2k_B T d_0}\right), \qquad (67)$$

which then shows a Brillouin function dependence with the magnetic field, the inverse of the temperature, as well as a linear dependence with the spin-aligner material thickness as observed experimentally.[11,13,14,33] Notice that instead of including the temperature dependence in the magnetic semiconductor g factor we have assumed this dependence in the phenomenological magnetization.[27] In Fig. 6 we plot the normalized polarization $P_j^* = P_j J_0 x/\bar{x}d_0\mathcal{G}_e'\mu_B$, i.e., $(d_{sm}/d_0)\mathcal{B}_{1/2}(\mathcal{G}_e'\mu_B B/2k_B T)$, as function of the magnetic field in Fig. 6(a) and the temperature in Fig. 6(b). These figures clearly show the observed injection polarization[11] by varying B, T, and the magnetic semiconductor spin-aligner thickness, justifying our pumping rate modeling through Eqs. (63) and (65).

C. Net light emission polarization

Now we can include the spin-aligned carrier injection, as described above, in the polarized light emission (60). The spin aligned carrier injection reflects as an unbalanced carrier population through Eq. (63). We must remark that due to the reduced spin-orbit coupling in the conduction band, spin injection of electrons is more efficient than holes. Thus we simply set a balanced constant pumping rate for holes from the drain lead, while considering an electronic spin-aligned injection. For the following calculations we fixed the temperature to $T = 4.2$ K, where the thermal photons emission is negligible, and thus can be simply disregarded from Eq. (60).

In working device regime radiative recombination rate is always much higher than nonradiative recombination rate as the former is dominant and the latter is a disturbance due to the impurities and other undesirable material defects. Thus nonradiative recombination rate is always smaller than pumping rate, even in the low injection limit. The radiative recombination rate, however, play a crucial role for the limiting regimes for the pump to recombination rate (69). First let us consider the regime of strong pumping rate where $\gamma_r^\mu \ll \Lambda_{\alpha\mathbf{k}}^\mu$. Thus $\Gamma_{\mathbf{k}}^{\mu\mu'}$ saturates to 1 and Eq. (60) simplifies to

$$\mathcal{P}(\nu_l) = \frac{\sum_{\mathbf{k}\mu\mu'} (\mu - \mu') |g_{l\mathbf{k}\mu\mu'}|^2 \mathcal{L}_{l\mathbf{k}}^{\mu\mu'}}{\sum_{\mathbf{k}\mu\mu'} |g_{l\mathbf{k}\mu\mu'}|^2 \mathcal{L}_{l\mathbf{k}}^{\mu\mu'}}, \quad (68)$$

which is a saturation for the emitted light polarization, since in that limit all the electronic and hole states are occupied, as follows from Eqs. (56) and (57), leaving no free state for carrier injection. The polarization is then dependent only on the spectral shape of the GaAs light emission and corresponds to the intrinsic emission we studied before, in the limit of high occupancy. On the other hand, for the regime of weak pumping, when $\gamma_r^\mu \gg \Lambda_{\alpha\mathbf{k}}^\mu$, the pumping to recombination rate reads

$$\Gamma_{\mathbf{k}}^{\mu\mu'} \equiv \frac{\Lambda_{e\mathbf{k}}^\mu \Lambda_{h-\mathbf{k}}^{\mu'}}{(\gamma_{NR}^\mu + \gamma_r^\mu)(\gamma_{NR}^{\mu'} + \gamma_r^{\mu'})} \ll 1, \quad (69)$$

which is the limit where all the electronic and hole states are almost unoccupied, due to the fast recombination process. In this situation the net light emission polarization is then strongly dependent on the polarized carrier injection, but with the GaAs light emission features. This limit is also consistent with the low injection limit we have taken before. The net spectral polarization is then given by

$$\mathcal{P}(\nu_l) = \frac{\sum_{\mathbf{k}\mu\mu'} (\mu - \mu') |g_{l\mathbf{k}\mu\mu'}|^2 \mathcal{L}_{l\mathbf{k}}^{\mu\mu'} f_{e\mathbf{k}0}[J_0/2 + \mu d_{MS}(\bar{x}/x)\mathcal{G}'_e \mu_B \mathcal{B}_{1/2}(\mathcal{G}'_e \mu_B B d_{MS}/2k_B T d_0)]}{\sum_{\mathbf{k}\mu\mu'} |g_{l\mathbf{k}\mu\mu'}|^2 \mathcal{L}_{l\mathbf{k}}^{\mu\mu'} f_{e\mathbf{k}0}[J_0/2 + \mu d_{Ms}(\bar{x}/x)\mathcal{G}'_e \mu_B \mathcal{B}_{1/2}(\mathcal{G}'_e \mu_B B d_{Ms}/2k_B T d_0)]}, \quad (70)$$

from where we obtain by integration the net light emission polarization as plotted in Fig. 7 by varying B and d_{MS}. Due to the low value of the Landé g-factor for electrons in GaAs, the Zeeman splitting is very small, but it is contrary to the splitting of the spin-aligner material, decreasing the polarization, which contributes to the decreasing of the saturation value for the net degree of polarization. Both the polarization of the spin-injected electrons (P_j) and that due to intrinsic g factor (P) increase in magnitude as the applied magnetic field increases, however, P_j is opposite to P. In our model P_j is dominant up to 7 T, where P_j saturates but P does not, therefore the net polarization drops as evidenced experimentally[11,13,14] (see the inset of Fig. 7). The spin-aligner material layer thickness is also an important feature for the net degree of polarization. We note that for this figure we have considered both light and heavy hole states, and thus the highest polarization possible to be attained is 50%. Had we neglected light-hole states the polarization could be as high as 100% depending on the spin-aligner material layer thickness. For $d_{MS} = 300$ nm the higher attained efficiency of polarization would be approximately 85%, which is in complete agreement with the observed value of 86% from Ref. 11.

VII. CONCLUDING REMARKS

In conclusion we have shown that the Langevin approach is quite useful for the microscopic description of spin-mediated polarized light emission. We have quantified the intrinsic degree of polarization of the GaAs light emission, being it strongly affected by temperature effects. We have shown that the temperature dependence of the electronic g factor is responsible for a slight decrease of the degree of polarization, once the decrease of the electronic g factor with the temperature decreases the conduction band spin-splitting sensitivity to the magnetic field. However, at higher temperatures, thermal photons are also emitted by the GaAs device, and the intrinsic degree of polarization decreases abruptly at the threshold temperature (T_c). The effect of unbalanced spin injection was also analyzed reflecting the dependence on the spin-aligned carrier pumping, as well as on the radiative and the nonradiative electron-hole recombination. Since the intrinsic polarization in GaAs is opposite to that in spin-polarizing materials, it decreases the net spin-injection efficiency as reported in Refs.[11,13,14] We have modeled the spin-polarized carrier injection by considering the spin aligner as
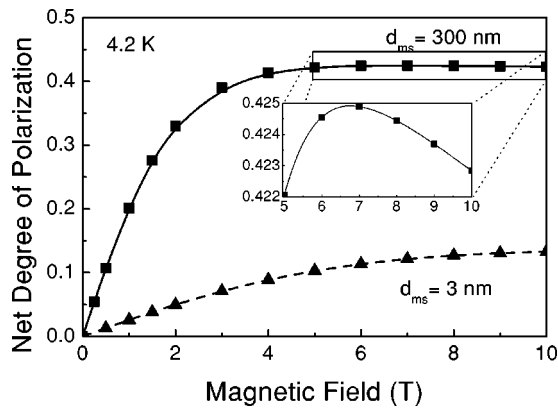
FIG. 7. Net light polarization with inclusion of spin-aligned carrier injection. The degree of light polarization is dependent on the magnetic material layer thickness. The inset shows the decrease of the saturated spin-aligned due to the intrinsic GaAs polarized light emission.

a Brillouin paramagnet,[27] and introduced a phenomenological spin-polarized current density, which is dependent on the spin-aligner layer thickness, the applied magnetic field and the temperature as well.

As a final remark, throughout this paper we have assumed the dipole quasiequilibrium regime for analyzing the light emission polarization. That means we have considered that each electronic spin component is in equilibrium inside each subband when radiative processes take place. This is actually the situation for working devices regime. However, the non-equilibrium regime, where the dipole dephasing and decoherence rate are taken into account, is interesting for the treatment of optical detection of spin relaxation processes.[18] The formalism here developed can be readily applied to these problems and could bring some enlightening on the microscopic mechanism related to spin relaxation in semiconductors media.

[1] S.A. Wolf, D.D. Awschalom, R.A. Buhrman, J.M. Daughton, S. von Molnr, M.L. Roukes, A.Y. Chtchelkanova, and D.M. Treger, Science **294**, 1488 (2001).

[2] S. Datta and B. Das, Appl. Phys. Lett. **56**, 665 (1990).

[3] G.A. Prinz, Science **282**, 1660 (1998); Phys. Today **48(4)**, 58 (1995).

[4] D.D. Awschalom and J.M. Kikkawa, Phys. Today **287**, 33 (1999).

[5] S. Das Sarma, J. Fabian, X. Hu, and I. Zutic, IEEE Trans. Magn. **36**, 2821 (2000).

[6] D. Loss and D.P. DiVicenzo, Phys. Rev. A **57**, 120 (1998).

[7] B.E. Kane, Nature (London) **393**, 133 (1998).

[8] M. Ostreich, Nature (London) **402**, 735 (1999).

[9] M. Ostreich et al., Appl. Phys. Lett. **74**, 1251 (1999).

[10] G. Schmidt, D. Ferrand, L.W. Molenkamp, A.T. Filip, and B.J. van Wees, Phys. Rev. B **62**, R4790 (2000).

[11] R. Fiederling, M. Kleim, G. Reuscher, W. Ossau, G. Schmidt, A. Waag, and L.W. Molenkamp, Nature (London) **402**, 787 (1999).

[12] Y. Ohno, D.K. Young, B. Beschoten, F. Matsukura, H. Ohno, and D.D. Aschalom, Nature (London) **402**, 790 (1999).

[13] B.T. Jonker, Y.D. Park, B.R. Bennett, H.D. Cheong, G. Kioseoglou, and A. Petrou, Phys. Rev. B **62**, 8180 (2000).

[14] B.T. Jonker, A.T. Hanbicki, Y.D. Park, G. Itskos, M. Furis, G. Kioseglou, A. Petrou, and X. Wei, Appl. Phys. Lett. **79**, 3098 (2001).

[15] J.C. Egues, Phys. Rev. Lett. **80**, 4578 (1998).

[16] Th. Gruber, M. Keim, R. Fiederling, G. Reuscher, W. Ossau, G. Schmidt, and L.W. Molenkamp, Appl. Phys. Lett. **78**, 1101 (2001).

[17] J.-B Xia, G.-Q. Hai, and J.N. Wang, Solid State Commun. (to be published).

[18] M. Oestreich and W.W. Rühle, Phys. Rev. Lett. **74**, 2315 (1995); M. Oestreich, S. Hallstein, A.P. Heberle, K. Eberl, E. Bauser, and W. Rühle, Phys. Rev. B **53**, 7911 (1996).

[19] W.W. Chow, S.W. Koch, and M. Sargent III, *Semiconductor-Laser Physics* (Spring-Verlag, Berlin, 1994).

[20] H. Fujisaki and A. Shimizu, Phys. Rev. A **57**, 3074 (1998).

[21] Y. Yamamoto, S. Machida, and O. Nilson, Phys. Rev. A **34**, 4025 (1986); Y. Yamamoto and S. Machida, *ibid.* **35**, 5114 (1987).

[22] G. Björk, Phys. Rev. A **45**, 8259 (1992).

[23] H. Haug and S.W. Koch, *Quantum Theory of the Optical and Electronic Properties of Semiconductors* (World Scientific, Singapore, 1990).

[24] D.F. Walls and G.J. Milburn, *Quantum Optics* (Springer-Verlag, Berlin, 1995).

[25] M.O. Scully and M.S. Zubairy, *Quantum Optics* (Cambridge University Press, Cambridge, 1997).

[26] C. W. Gardiner, and P. Zoller, *Quantum noise: a handbook of Markovian and Non-Markovian Quantum Stochastic Methods with Applications to Quantum Optics* (Springer, Berlin, 2000).

[27] J.K. Furdyna, J. Appl. Phys. **64**, R29 (1998).

[28] T. Fukumura, Z. Jin, M. Kawasaki, T. Shono, T. Hasegawa, S. Koshihara, and H. Koinuma, Appl. Phys. Lett. **78**, 958 (2001).

[29] B.K. Ridley, *Quantum Processes in Semiconductors* (Oxford University Press, New York, 1993).

[30] M.W. Wu and H. Metiu, Phys. Rev. B **61**, 2945 (2000).

[31] C.W. Gardiner and M.J. Collett, Phys. Rev. A **31**, 3761 (1985).

[32] E.L. Dereniak and D.G. Crowe, *Optical Radiation Detectors* (Wiley, New York, 1984).

[33] H.J. Zhu, M. Ramsteiner, H. Kostial, M. Wassermeier, H.-P. Schönherr, and K.H. Ploog, Phys. Rev. Lett. **87**, 016601 (2001).

[34] We note that although the employed model be considered inside the working device regime, i.e., for "good" devices, where the radiative recombination rate is always much higher than nonradiative recombination rate due to phonon scattering, the observed behavior is still valid outside this regime. Phonon scattering will cope with the radiative thermal effect on decreasing the intrinsic light emission degree of polarization.